

Flexible Tails for Normalizing Flows

Tennessee Hickling
School of Mathematics
University of Bristol
Bristol, UK

TENNESSEE.HICKLING@BRISTOL.AC.UK

Dennis Prangle
School of Mathematics
University of Bristol
Bristol, UK

DENNIS.PRANGLE@BRISTOL.AC.UK

Abstract

Normalizing flows are a flexible class of probability distributions, expressed as transformations of a simple base distribution. A limitation of standard normalizing flows is representing distributions with heavy tails, which arise in applications to both density estimation and variational inference. A popular current solution to this problem is to use a heavy tailed base distribution. Examples include the tail adaptive flow (TAF) methods of Laszkiewicz et al. (2022). We argue this can lead to poor performance due to the difficulty of optimising neural networks, such as normalizing flows, under heavy tailed input. This problem is demonstrated in our paper. We propose an alternative: use a Gaussian base distribution and a final transformation layer which can produce heavy tails. We call this approach tail transform flow (TTF). Experimental results show this approach outperforms current methods, especially when the target distribution has large dimension or tail weight.

Keywords: normalizing flows, extreme values, heavy tails, variational inference

1 Introduction

A normalizing flow (NF) expresses a complex probability distribution as a parameterised transformation of a simpler base distribution. A NF sample is

$$x = T(z; \theta), \tag{1}$$

where z is a sample from the base distribution, typically $\mathcal{N}(0, I)$. A number of transformations have been proposed which produce flexible and tractable distributions. Typically multiple transformations are composed to form T with the desired level of flexibility. Applications include density estimation (fitting a transformation to observed data points) and variational inference (fitting a transformation to a target distribution). In either case θ , the parameters controlling T , can be optimised using stochastic gradient methods for a suitable objective function. For reviews of NFs see Kobyzev et al. (2020) and Papamakarios et al. (2021).

Modelling distributions with heavy tails is critical in many applications such as climate (Zscheischler et al., 2018), contagious diseases (Cirillo and Taleb, 2020) and finance (Gilli and K ellezi, 2006). Indeed, in the context of density estimation, results from extreme value theory (EVT) (Coles, 2001; Embrechts et al., 2013) show distributional tails can often be modelled using a particular heavy tailed distribution, the generalized Pareto distribution

(GPD). Heavy tailed targets can also arise naturally in Bayesian inference, requiring heavy tailed approximate distributions in variational inference (Liang et al., 2022) (and providing challenges for MCMC methods—see e.g. Yang et al., 2022).

However standard normalizing flows do not model heavy tails well. In particular, Jaini et al. (2020) prove that Gaussian tails cannot be mapped to GPD tails under Lipschitz transformations. (This is a special case of their main result, which we present as Theorem 2 below.) Many normalizing flows use Lipschitz transformations of Gaussian base distributions, implying they produce distributions which are poor approximations of heavy tailed distributions.

Based on this result, several authors have proposed using heavy tailed base distributions. This includes the **tail adaptive flow** (TAF) methods of Laszkiewicz et al. (2022) for density estimation, and similar methods for variational inference (Liang et al., 2022). We argue that using heavy tailed base distributions has an important drawback. Typical NF transformations involve passing the input z through a neural network. However neural network optimisation can perform poorly under heavy tailed input—as this can induce heavy tailed gradients, which are known to be problematic (Zhang et al., 2020). We verify this problem empirically, first in Section 4.1 for a simple neural network regression example, and then in Section 4.2 for normalizing flows.

To improve performance we propose an alternative approach: use a Gaussian base distribution with a final non-Lipschitz transformation in T . We refer to this as the **tail transform flow** (TTF) approach. The difference is represented schematically in Figure 1. In Section 3.1 we provide a suitable final transformation (3), which is motivated by extreme value theory. This is easy to implement in automatic differentiation libraries as it’s based on a standard special function: the complementary error function. We also prove that this transformation converts Gaussian tails to heavy tails with tunable tail weights, and hence provides the capability of producing heavy tails when used with standard flows.

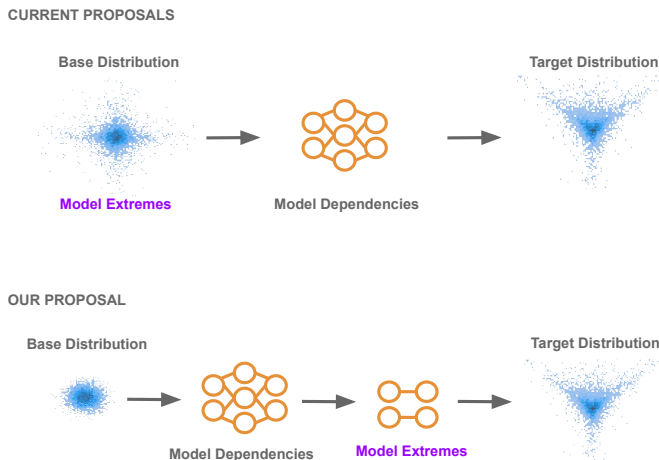


Figure 1: Our proposed method changes the location where extremes/tails are modelled.

We perform experiments which show our TTF approach outperforms current methods, especially when the target distribution has large dimension or tail weight. We concen-

trate on density estimation, investigating both synthetic and real data. A proof-of-concept variational inference experiment is also included.

To summarise, our contributions are:

- We illustrate the problem of using extreme inputs in (a) generic neural networks (b) normalizing flows.
- We introduce the TTF transformation—equation (3) below—and prove results to show it converts Gaussian tails to heavy tails with tunable tail weights. This provides the capability of producing heavy tails when used with standard NFs.
- We provide practical methodology to use TTF in a normalizing flow architecture.
- We demonstrate improved empirical results for density estimation (synthetic and real data examples) and variational inference (a proof-of-concept example with an artificial target) compared to standard normalizing flows, and other NF methods for heavy tails.

In the remainder of this section we review related prior work. Then Section 2 outlines background material and Section 3 describes our proposed transformation, as well as summarising our theoretical results. Section 4 contains our examples, and Section 5 concludes. The appendices contain further technical details, including proofs. Code for all our examples can be found at <https://github.com/tennessee-wallaceh/tailnflows>.

1.1 Related Work

1.1.1 THEORY

A common definition of heavy tails (e.g. Foss et al., 2011) is as follows.

Definition 1 *A real valued random variable Z is (right-)heavy-tailed when $\mathbb{E}[\exp(\lambda Z)] = \infty$ for all $\lambda > 0$. Otherwise Z is **light-tailed**.*

Examples of heavy tailed distributions include Student’s T and Pareto distributions. An example of a light tailed distribution is the Gaussian distribution. Jaini et al. (2020) prove the following result.

Theorem 2 *Let Z be a light tailed real valued random variable and T be a Lipschitz transformation. Then $T(Z)$ is also light tailed.*

In further results Jaini et al. derive the gradient that T requires to produce desired tail-properties, and generalise their results to the multivariate case. Finally they also prove that several popular classes of NFs use Lipschitz transformations (see also Liang et al., 2022).

Other mathematical definitions of tail behaviour exist, including alternative usages of the term “heavy tails”. Liang et al. (2022) apply such definitions to prove more detailed results on how Lipschitz transformations affect tail weights (e.g. Theorem 10 in our appendices).

To model heavy tailed distributions, Jaini et al. note that there is a choice “of either using source densities with the same heaviness as the target, or deploying more expressive transformations than Lipschitz functions”. They pursue the former approach and this paper investigates the latter.

1.1.2 HEAVY TAILED BASE DISTRIBUTIONS

Several NF papers propose using a heavy tailed base distribution. To discuss these, let Z be a random vector following the base distribution of the normalizing flow, and let Z_i be its i th component.

Firstly, in the setting of density estimation, Jaini et al. (2020) set $Z_i \sim t_\nu$: a standard (location zero, scale one) Student’s T distribution with ν degrees of freedom. The Z_i components are independent and identically distributed. The ν parameter is learned jointly with the NF parameters. Optimising their objective function requires evaluating the Student’s T log density and its derivative with respect to ν , which is straightforward.

An extension is to allow **tail anisotropy**—tail behaviour varying across dimensions—by setting (independently) $Z_i \sim t_{\nu_i}$, so the degrees of freedom can differ with i . In Laszkiewicz et al. (2022), two such approaches are proposed for density estimation. Marginal Tail-Adaptive Flows (mTAF) first learn ν_i values using a standard estimator (a version of the Hill, 1975 estimator). Then the distribution of Z is fixed while learning T . Another feature of mTAF is it allows Gaussian marginals by using Gaussian base distributions for appropriate Z_i components, and then keeping Gaussian and non-Gaussian components separate throughout the flow. Generalised Tail-Adaptive Flows (gTAF) train the ν_i s and θ jointly. Liang et al. (2022) propose a similar method to gTAF for the setting of variational inference: Anisotropic Tail-Adaptive Flows (ATAF).

1.1.3 OTHER METHODS

Here we discuss work on alternatives to a Student’s T base distribution. In the setting of density estimation, Amiri et al. (2022) consider two alternative base distributions: Gaussian mixtures, and generalized Gaussian. For the former, they argue that mixture distributions can in theory model any smooth density given enough components, and also that they are more stable in optimisation than heavy tailed base distributions. The latter has tails which can be heavier than Gaussian, but are lighter than Student’s T.

McDonald et al. (2022) propose COMET (copula multivariate extreme) flows for the setting of density estimation. This involves a preliminary stage of estimating marginal cumulative distribution functions (cdfs) for each component of the data. The body of each marginal is approximated using kernel density estimation, and the tails are taken as GPDs, with shape parameters chosen using maximum likelihood. The COMET flow then uses a Gaussian base distribution, followed by a **copula transformation**. This is an arbitrary normalizing flow followed by an elementwise logistic transformation so that output is in $[0, 1]^d$. Finally the inverse marginal cdfs are applied to each component. In Appendix B.2 we analyse the resulting tail behaviour and prove that the output cannot capture the full range of heavy tailed behaviour. (More formally, Theorem 11 proves that the output is not in the Fréchet domain of attraction, which is defined in Section 2.4.) Despite this our experiments in Section 4 find COMET flows often have good empirical performance, which we discuss in Section 5.

The extreme value theory literature also proposes methods to jointly model heavy tails and the body of a distribution. See Huser et al. (2024) (Section 4) for a review of several approaches. We comment on one particularly relevant method: Papastathopoulos and Tawn (2013); Naveau et al. (2016); de Carvalho et al. (2022) use a cdf $G \circ H(y)$ which

composes the GPD cdf H with a **carrier function** $G : [0, 1] \rightarrow [0, 1]$ which is taken to be a simple parametric function. Similarly, Stein (2021) composes several carrier functions. Our approach is similar, effectively using normalizing flows in place of carrier functions, and covering the multivariate case. Naveau et al. (2016) proves that certain conditions on the carrier function provide useful theoretical properties, and it would be interesting to explore analogous results for our method in future.

2 Background

2.1 Normalizing Flows

Consider vectors $z \in \mathbb{R}^d$ and $x = T(z) \in \mathbb{R}^d$. Suppose z is a sample from a base density $q_z(z)$. Then the transformation T defines a **normalizing flow** density $q_x(x)$. Suppose T is a diffeomorphism (a bijection where T and T^{-1} are differentiable), then the standard change of variables formula gives

$$q_x(x) = q_z(T^{-1}(x)) |\det J_{T^{-1}}(x)|. \quad (2)$$

Here $J_{T^{-1}}(x)$ denotes the Jacobian of the inverse transformation and \det denotes determinant.

Typically a parametric transformation $T(z; \theta)$ is used, and $q_z(z)$ is a fixed density, such as that of a $\mathcal{N}(0, I)$ distribution. However some previous work uses a parametric base density $q_z(z; \theta)$. (So θ denotes parameters defining both T and q_z .) For instance several methods from Section 1.1 use a Student's T base distribution with variable degrees of freedom.

Usually we have $T = T_K \circ \dots \circ T_2 \circ T_1$, a composition of several simpler transformations. Many such transformations have been proposed, with several desirable properties. These include producing flexible transformations and allowing evaluation (and differentiation) of T , T^{-1} , and the Jacobian determinant. Such properties permit tractable sampling via (1), and density evaluation via (2).

Throughout the paper we describe NFs in the **generative direction**: by defining the transformations T_i applied to a sample from the base distribution. NFs can equivalently be described in the **normalizing direction** by defining the T_i^{-1} transformations. We pick the generative direction simply to be concrete.

2.2 Density Estimation

Density estimation aims to approximate a target density $p(x)$ from which we have independent samples $\{x_i\}_{i=1}^N$. We assume $x_i \in \mathbb{R}^d$.

We can fit a normalizing flow by minimising the objective

$$\mathcal{J}_{\text{DE}}(\theta) = - \sum_{i=1}^N \log q_x(x_i; \theta).$$

This is equivalent to minimising a Monte Carlo approximation of the Kullback-Leibler divergence $KL[p(x)||q_x(x; \theta)]$. The objective gradient can be numerically evaluated using automatic differentiation. Thus optimisation is possible by stochastic gradient methods. This approach remains feasible under a Student's T base distribution as its log density and required derivatives are tractable.

2.3 Variational Inference

Variational inference (VI) aims to approximate a target density $p(x)$, often a Bayesian posterior for parameters $x \in \mathbb{R}^d$. Typically VI is used where only an unnormalised target $\tilde{p}(x)$ can be evaluated. Then $p(x) = \tilde{p}(x)/\mathcal{Z}$ but the normalizing constant $\mathcal{Z} = \int_{\mathbb{R}^d} \tilde{p}(x)dx$ cannot easily be calculated.

VI aims to minimise $KL[q_x(x; \theta)||p(x)]$ over a parameterised set of densities $q_x(x; \theta)$. In this paper $q_x(x; \theta)$ is a normalizing flow. An equivalent optimisation task is maximising the **ELBO** objective

$$\mathcal{J}_{\text{VI}}(\theta) = \mathbb{E}_{x \sim q_x}[\log \tilde{p}(x) - \log q_x(x; \theta)].$$

This has a tractable unbiased gradient estimate

$$M^{-1} \sum_{i=1}^M \nabla_{\theta}[\log \tilde{p}(x_i) - \log q_x(x_i; \theta)],$$

where $x_i = T(z_i; \theta)$ and $\{z_i\}_{i=1}^M$ are independent samples from the base distribution. Again, the gradient estimate can be numerically evaluated using automatic differentiation, allowing optimisation by stochastic gradient methods.

A generalisation of the above is to use a base distribution with parameters. In particular, ATAF (Liang et al., 2022) needs to learn degrees of freedom for Student’s T distributions. The above approach remains feasible by using a Student’s T sampling scheme which allows application of the reparameterization trick, as detailed in Appendix D.2.

For more background on this form of variational inference see Rezende and Mohamed (2015); Blei et al. (2017); Murphy (2023).

2.4 Extreme Value Theory

Extreme value theory (EVT) is the branch of statistics studying extreme events (Coles, 2001; Embrechts et al., 2013). A classic result is **Pickands theorem** (Pickands III, 1975); see Papastathopoulos and Tawn (2013) for a review. Given a scalar real-valued random variable X , consider the scaled excess random variable $\frac{X-u}{h(u)} | X > u$, where $u > 0$ is a large threshold and $h(u) > 0$ is an appropriate scaling function. The theorem states that if the scaled excess converges in distribution to a non-degenerate distribution, then it converges to a Generalized Pareto distribution (GPD).

A common EVT approach is to fix some u , treat $h(u)$ as constant, and model tails of distributions as having GPD densities. The motivation is that this should be a good tail approximation near to u , while for $x \gg u$ there is not enough data to estimate the behaviour of $h(u)$.

The GPD distribution involves a shape parameter, $\lambda \in \mathbb{R}$. For $\lambda > 0$, the GPD density is asymptotically (for large x) proportional to $x^{-1/\lambda-1}$, while for $\lambda < 0$ the upper tail has bounded support. In terms of Definition 1, $\lambda > 0$ guarantees heavy tails and $\lambda < 0$ guarantees light tails. Given X , the shape parameter of the GPD resulting from Pickands theorem is a measure of how heavy the tail of X is. A Gaussian distribution results in $\lambda = 0$ (and requires a non-constant scaling function $h(u)$), and $\lambda > 0$ represents heavier tails. Finally, we will use the following definition in our theoretical results later.

Definition 3 *The **Fréchet domain of attraction** with shape parameter λ , Θ_λ is the set of distributions resulting in $\lambda > 0$ under Pickands theorem.*

3 Methods and Theory

We propose producing normalizing flow samples $R \circ T_{\text{body}}(z)$, where z is a $\mathcal{N}(0, 1)$ sample and T_{body} is a standard normalizing flow transformation, and R is defined shortly. If T_{body} is a Lipschitz transformation, then the input to R has light tails by Theorem 2. Thus the resulting architecture avoids the problem of passing extreme values as inputs to any neural network layers. The final transformation R should be able to output heavy tails of any desired tail weight. This section presents our proposal for a suitable transformation R .

Section 3.1 describes our proposed transformation for the univariate case, and summarises our theoretical results on its tail behaviour (with full details in the appendices). Sections 3.2–3.4 give further details to produce a practical general-purpose method. Technical details are included in the appendices. This includes a discussion of alternative transformations and related results in the literature, in Appendix C.

3.1 TTF Transformation

We propose the **tail transform flow** (TTF) transformation $R : \mathbb{R} \rightarrow \mathbb{R}$,

$$R(z; \lambda_+, \lambda_-) = \mu + \sigma \frac{s}{\lambda_s} [\text{erfc}(|z|/\sqrt{2})^{-\lambda_s} - 1]. \quad (3)$$

We use the notation $s = \text{sign}(z)$, with $\lambda_s = \lambda_+$ for $s = 1$ and $\lambda_s = \lambda_-$ for $s = -1$. The transformation is based on erfc , the **complementary error function**. This is a special function, reviewed in Appendix A.1, which is tractable for use in automatic differentiation using standard libraries. The parameters $\lambda_+ > 0, \lambda_- > 0$ control tail weights for the upper and lower tails, allowing us to capture tail weight asymmetry in these two tails. The parameters $\mu \in \mathbb{R}$ and $\sigma > 0$ are location and scale parameters. We found these helped performance, although similar effects could be achieved in principle by adjusting T_{body} .

To perform density evaluation via (2) we need to evaluate the inverse and derivative of (3). These, and some other properties, are provided in Appendix A.3.

Composing R with existing normalizing flows permits the output to have heavy tails with parameterised weights. This is shown by the following argument. Most normalizing flows use a Gaussian base distribution and a Lipschitz transformation. By Theorem 2 the output has light tails. Since the NF transformation can be the identity, it is capable of producing Gaussian tails. A property of (3) is that if X has Gaussian tails, then $R(X)$ is in the Fréchet domain of attraction (see Definition 3) with λ_+, λ_- controlling the tail shape parameters. A special case is that $\mathcal{N}(0, 1)$ tails produce GPD output with shape parameters λ_+, λ_- . These properties are proved in Appendix B.3 (Theorem 12).

3.2 Multivariate Transformation

Here we discuss extending our univariate transformation $R : \mathbb{R} \rightarrow \mathbb{R}$ to the multivariate case. In this paper we follow the simple approach of transforming each marginal with its own $\mu, \sigma, \lambda_+, \lambda_-$ parameters. In some cases it can be known that a particular marginal is

light tailed. Then we could simply perform an identity transformation instead. However, in practice we find that in such cases fixing λ_+, λ_- to low values (in particular $\lambda = 1/1000$) suffices.

A more flexible approach would be to allow dependence, for instance by using an autoregressive structure (Papamakarios et al., 2021) to generate the λ_+, λ_- parameters for each marginal. This could capture tail behaviour that varies in different parts of the distribution. However, exploratory work found that this approach is harder to optimise, so we leave it for future research.

3.3 Tail Parameter Initialisation

The initialisation of the tail parameters λ_+, λ_- is often important to the stability of the method. For density estimation in the presence of heavy tailed data, the parameters must be initialised sufficiently high, such that large observations are not mapped to vanishingly low probability regions of the base distribution. If this does occur, it is possible to get numerical overflow during optimisation. For variational inference a related problem can occur. If some tail parameters are too high, then we can sample points of very low target density and get numerical overflow. In practice, we find that initialising λ uniformly from $[0.05, 1]$ provides sufficient stability.

3.4 Two Stage Procedure

As discussed in Section 3.3, joint optimisation of R and T_{body} can require careful initialisation of the λ parameters. As an alternative, we propose a two stage procedure for density estimation: TTF fix. Here the tail weight λ_-, λ_+ parameters of R are estimated in an initial step and then fixed while optimising T_{body} (and the μ, σ parameters of R .) This can be viewed as first transforming the data using R to remove heavy tails, and then fitting a standard normalizing flow to the transformed data. Similar approaches appear in McDonald et al. (2022) and Laszkiewicz et al. (2022).

Shape parameter estimators exist in the EVT literature, which we can apply to each marginal tail. We follow Laszkiewicz et al. (2022) in using the Hill double-bootstrap estimator (Danielsson et al., 2001; Qi, 2008). McDonald et al. (2022) perform maximum likelihood estimation on the highest and lowest 5% of data, to produce tail parameters for the positive and negative tails respectively.

We do not consider a similar two stage procedure for VI. This is because preliminary estimation of tail weights from the unnormalised target distribution is not straightforward. However recent work on static analysis of probabilistic programs (Liang et al., 2024) provides progress in this direction.

4 Experiments

This section contains our empirical experiments. Firstly, recall that one motivation for our work in Section 1 is the claim that neural network optimisation can perform poorly under heavy tailed inputs. We verify this empirically in Section 4.1 for a simple neural network regression example, and then in Section 4.2 for normalizing flows. Secondly, Sections 4.2–4.4 contain normalizing flow examples, comparing our method to existing approaches

d	ν	Sigmoid activation	ReLU activation
5	30.0	1.01 (1.02)	1.01 (1.04)
	2.0	1.74 (6.19)	1.06 (1.08)
	1.0	1.57e+03 (8.57e+06)	3.45 (1.93e+03)
10	30.0	1.02 (1.02)	1.02 (1.05)
	2.0	2.04 (7.28)	1.03 (1.05)
	1.0	4.13e+03 (1.09e+06)	8.41 (49.6)
50	30.0	1.01 (1.04)	1.08 (1.09)
	2.0	3.09 (5.26)	1.27 (12.3)
	1.0	1.03e+04 (1.73e+06)	55.8 (6.59e+03)
100	30.0	1.02 (1.07)	1.15 (1.2)
	2.0	3.41 (4.33)	1.60 (1.74)
	1.0	1.02e+05 (1.94e+05)	336 (1.2e+03)

Table 1: Results of the neural network regression example. Values are the median test MSE over 5 trials, with the maximum provided in brackets. (We use median as it’s more robust than mean to extreme outliers. Maximum illustrates the presence and magnitude of such outliers.)

for density estimation and a proof-of-concept variational inference example. Additional implementation details are provided in Appendix D.

4.1 Neural Network Regression with Extreme Inputs

This experiment considers the following simple regression problem

$$\{X_i\}_{i=1}^d \sim t_\nu, \quad Y \sim \mathcal{N}(X_d, 1).$$

The d -dimensional input is heavy tailed. The output equals one of the inputs plus Gaussian noise.

Experimental Details We consider a number of tail weight (ν) and dimension (d) combinations, generating 5000 train, validation and test samples for each. Our models are simple 2 layer multi-layer perceptrons with 50 nodes in each hidden layer. The models are optimised with Adam to minimise mean square error, selecting the model with smallest validation loss found during training. We consider both sigmoid and ReLU activations. This is to investigate whether the main issue is saturation of sigmoid activation functions. The experiment was repeated 5 times, each trial sampling a new set of data.

Results Table 1 shows the results of the experiment. Both models perform well for $\nu = 30$ (light tailed inputs), worse for $\nu = 2$, and very badly for $\nu = 1$. Performance also decays as d increases, but the effect is weaker. The ReLU activation function performs a little better overall, but can still result in very large MSE values.

Overall, the results demonstrate the failure of neural network methods to capture a simple relationship in the presence of heavy tailed inputs. The problem persists under a

ReLU activation function, showing that it is not caused solely by saturation of the sigmoid activation function.

4.2 Density Estimation with Synthetic Data

This experiment looks at density estimation for data generated from the following model, with $d > 1$:

$$\{X_i\}_{i=1}^{d-1} \sim t_\nu, \quad X_d|X_{d-1} \sim \mathcal{N}(X_{d-1}, 1). \quad (4)$$

In this model the only non-trivial dependency to learn is between X_d and X_{d-1} , but there are also several heavy tailed nuisance variables.

We use this example to investigate whether modelling tails in the final layer of a NF is superior to modelling the tails in the base distribution. We look at how performance varies with changes in dimensionality d and tail weight ν . Section 4.1 showed that neural network regression can perform poorly under heavy tailed inputs. Here we investigate whether a similar finding holds in the setting of normalizing flows.

Some of the NF methods we compare involve fixed tail weight parameters (either ν for a Student’s T base distribution or λ_+, λ_- for our transformation), and for this experiment we fix these to their known true values. This means our analysis is not confounded by the difficulty of estimating these parameters. The tail weights are known as the marginal density for each X_i is asymptotically proportional to $x_i^{-\nu-1}$. (This can be shown for X_d by representing its density as a convolution and looking at the asymptotic behaviour.) Note that only λ_+, λ_- in (3) are fixed, not μ and σ .

Flow Architectures We investigate a selection of NF methods, including several which aim to address extremes. To conduct a fair comparison, we maintain as much consistency between the flow architectures as possible.

A baseline method, **normal**, uses a d -dimensional isotropic Gaussian base distribution. This is followed by an autoregressive rational quadratic spline layer then an autoregressive affine layer. The affine layer should be capable of capturing linear dependency, whilst the spline layer can adjust the shape of the body, but not the tails of the distribution.

Our proposed approach, tail transform flow, modifies the architecture just described by adding an additional layer for dealing with the tails, as described in Section 3. **TTF** trains the tail parameters alongside the other parameters. **TTF (fix)** is a 2-stage approach, which fixes the tail parameters to the known true values.

Marginal tail adaptive flows (**mTAF**) have the same architecture as **normal**, but use a Student’s T base distribution, as detailed in Section 1.1. The degrees of freedom are fixed to the correct tail parameters. Generalised tail adaptive flows (**gTAF**) differ in that the degrees of freedom are optimised alongside all other parameters during the training procedure.

As further variations on **normal**, we consider two alternative base distributions suggested by Amiri et al. (2022). The first is a Gaussian mixture model base distribution (**m_normal**) with 5 components (preliminary work found 10 or 15 components had no significant difference in performance). For each component we optimise the d dimensional mean and diagonal covariance terms along with other parameters. The second base distribution is d independent generalised normal distributions (**g_normal**). The generalised

normal family does not have Pareto tails, so we cannot fix them to have the true tail weight. Instead, we optimise the shape parameter of each marginal.

We also consider COMET flows (**COMET**), as detailed in Section 1.1. For the normalizing flow part of this method we use the same architecture as **normal**. Our analysis is based on the code of McDonald et al. (2022). We don't report results for $d = 50$ as we found the code extremely slow to run in this case (discussed further in Appendix F). COMET is a 2-stage approach, which involves estimating tail parameters in the first stage, so again we fix these to the known correct values.

Experimental Details We run 10 repeats for each flow/target combination. Each repeat samples a new set of data, with 5000 observations. which is split in proportion 40/20/40, to give training, validation and test sets respectively. We train using the Adam optimiser with a learning rate of 5e-3. We use an early stopping procedure, stopping once there has been no improvement in validation loss in 100 epochs, and returning the model from the epoch with best validation loss. The loss plots from the optimisation were also visually inspected to confirm convergence. The selected model is then evaluated on the test set to give a negative test log likelihood per dimension, reported below for a range of dimensions and tail weights. Dividing by dimension acts to normalises the metric, allowing for easier comparison across dimensions.

Results Table 2 shows the results. For near-Gaussian tails ($\nu = 30$) all methods perform similarly. The methods which are not specifically designed to permit GPD tails (normal, m_normal, g_normal) are the worst performing for $\nu \leq 2$, often not converging at all.

Fewer methods produce competitive results for heavier tails (small ν) and higher dimensions (large d). Only TTF, TTF (fix) and mTAF are always competitive. COMET is also competitive for $d < 50$, however it was not feasible to run it for $d = 50$. In general COMET outperforms mTAF, and the TTF methods outperform COMET. We did not detect a significant difference between the two TTF methods.

Overall, the results suggest that it is advantageous to model tails in the final transformation (TTF, TTF (fix), COMET). Another question is whether it's better to fix the tail parameters or optimise them. We found no significant difference here for TTF methods. However, since mTAF outperforms gTAF, fixing tail parameters is better for heavy tailed base distribution methods.

4.3 Density Estimation with S&P 500 Data

This section considers financial return data as an example of high dimensional multivariate data with extreme values. Our experiments target a varying number of dimensions $d \in \{100, 200, 300\}$, with data covering the time period 2010-01-04 to 2022-10-27, corresponding to 3227 days in total. For a given d , we take the closing prices of the top d most traded S&P 500 stocks, and convert them in standard fashion to log returns i.e. the log returns are $x_j = \log(\frac{s_{j+1}}{s_j})$ where s_j is stock closing price on day j . In this example we concentrate on the tails of the data, rather than time series structure. As such, we treat each day of log returns as an independent observation in \mathbb{R}^d . We normalize the log returns to zero mean and unit variance using the estimated mean and variance from the training and validation

d	Flow	$\nu = 0.5$	$\nu = 1$	$\nu = 2$	$\nu = 30$
5	normal	-	-	2.01 (0.07)	1.46 (0.00)
	m_normal	-	403.24 (239.15)	1.94 (0.02)	1.46 (0.00)
	g_normal	-	-	1.93 (0.01)	1.46 (0.00)
	gTAF	6.42 (0.27)	2.49 (0.02)	1.90 (0.01)	1.46 (0.00)
	TTF	3.33 (0.01)	2.34 (0.01)	1.89 (0.01)	1.47 (0.00)
	mTAF	4.08 (0.03)	2.49 (0.02)	1.92 (0.01)	1.46 (0.00)
	TTF (fix)	3.33 (0.01)	2.35 (0.01)	1.89 (0.01)	1.47 (0.00)
	COMET	3.42 (0.01)	2.35 (0.01)	1.89 (0.00)	1.46 (0.00)
10	normal	-	-	2.00 (0.02)	1.46 (0.00)
	m_normal	-	-	2.04 (0.07)	1.46 (0.00)
	g_normal	-	-	1.98 (0.02)	1.46 (0.00)
	gTAF	7.13 (0.31)	2.63 (0.02)	1.95 (0.00)	1.47 (0.00)
	TTF	3.55 (0.01)	2.47 (0.00)	1.93 (0.00)	1.47 (0.00)
	mTAF	4.48 (0.04)	2.63 (0.01)	1.95 (0.00)	1.46 (0.00)
	TTF (fix)	3.54 (0.01)	2.46 (0.00)	1.93 (0.00)	1.47 (0.00)
	COMET	3.63 (0.01)	2.46 (0.00)	1.93 (0.00)	1.47 (0.00)
50	normal	-	-	2.02 (0.01)	1.47 (0.00)
	m_normal	-	-	2.02 (0.00)	1.47 (0.00)
	g_normal	-	-	2.01 (0.00)	1.47 (0.00)
	gTAF	7.49 (0.38)	2.65 (0.01)	1.99 (0.00)	1.47 (0.00)
	TTF	3.68 (0.00)	2.54 (0.00)	1.98 (0.00)	1.47 (0.00)
	mTAF	5.22 (0.04)	2.62 (0.01)	1.98 (0.00)	1.47 (0.00)
	TTF (fix)	3.68 (0.00)	2.54 (0.00)	1.98 (0.00)	1.47 (0.00)

Table 2: Density estimation results on synthetic example. Each entry is a mean value of negative test log likelihood per dimension across 10 repeated experiments, with the standard error in brackets. Bold indicates methods whose mean log likelihood differs from the best mean by less than 2 standard errors (of the best mean). A dash indicates that the method did not converge (output was Inf or NaN) in at least one repeat.

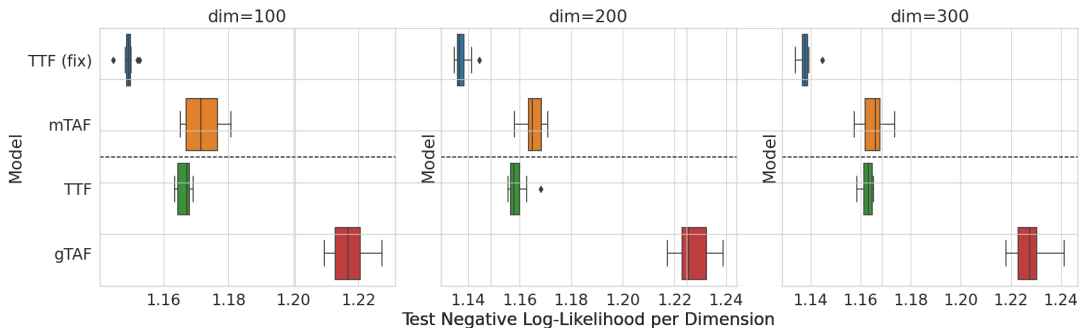


Figure 2: Box plot of test negative log likelihoods per dimension from fitting S&P 500 log returns (10 repeats). Results above the dashed line use a two-stage procedure.

sets, as is standard practice in NF density estimation. For example, see the experimental framework of Papamakarios et al. (2017) and Durkan et al. (2019).

Preliminary analysis confirmed that the resulting data does exhibit heavy tails in the marginal distributions.

Flow Architectures In this experiment we compare some NF architectures which performed reasonably well in Section 4.2: TTF, TTF (fix), mTAF and gTAF. It wasn’t feasible for us to run COMET flows for a problem of this dimension.

We reuse the NF architectures described in Section 4.2 with a slight alteration. We add trainable linear layers based on the LU factorisation (Oliva et al., 2018). For TTF methods, this immediately precedes the TTF layer. Otherwise, this is the final layer. The LU layers were included as we found that they greatly improved empirical performance.

See Section 3.4 for details of our initial stage of tail parameter estimation. Equivalent tail parameters are used for mTAF and TTF (fix). In some cases, this estimation procedure finds that a marginal distribution is light tailed. In these cases, as mentioned in Section 3.2, we set the tail parameter to a small value, corresponding to a degree of freedom of $\nu = 1000$.

Experimental Details We run 10 repeats for each flow/target combination. Each trains for 400 epochs using the Adam optimiser with a learning rate of $5e-4$. The test set is comprised of observations after 2017-09-14, with train and validation sampled uniformly from the period up to and including this date. This corresponds to 1292 training, 645 validation and 1290 test observations respectively. We perform a standard early stopping procedure, with the final model chosen as that which achieved the lowest loss on the validation set.

Results The results are presented in Figure 2. As in Section 4.2, the TTF methods outperform the heavy tailed base distribution methods, although the advantage of TTF over mTAF is small. However, now fixing the tail parameters is advantageous for all methods: TTF (fix) significantly outperforms TTF, and mTAF outperforms gTAF.

4.4 Variational Inference for Artificial Target

Here we consider variational inference using the target distribution (4). We previously used this in Section 4.2 to generate synthetic data for density estimation. As in that experiment, this model allows us to easily vary both target tail weights (ν) and number of nuisance variables (d).

Flow Architectures We compare four flows which exhibited good performance in Section 4.2: **TTF**, **TTF fix**, **mTAF** and **gTAF**. COMET flows also performed well in the density estimation setting. However they involve making kernel density estimates of marginal distributions, which has no obvious equivalent for the VI setting. So we do not include them in this comparison. As in Section 4.2, for TTF fix and mTAF we fix the tail parameters to the known correct values.

Although mTAF and gTAF were proposed as density estimation methods, it is straightforward to use these heavy tail base distribution methods for this VI task. As noted earlier, gTAF (Laszkiewicz et al., 2022) is equivalent to ATAF (Liang et al., 2022) in the context of variational inference, and trains the tail parameters alongside the other parameters. It is difficult to apply mTAF to VI in general, due to the difficulty of estimating the tail parameters, but in this case we have theoretical correct values.

Experimental Details We consider $\nu \in \{1, 2, 30\}$, which covers; Cauchy, lighter than Cauchy and close to Gaussian nuisance noise respectively. (Unlike Section 4.2, we do not consider $\nu = 0.5$ as $\nu = 1$ already produces a clear conclusion of a single best method.) Additionally, we consider $d \in \{5, 10, 50\}$. We run 5 repeats for each flow/target combination. Each repeat uses 10,000 iterations of the Adam optimiser using a learning rate of 1e-3. The loss plots from the optimisation were visually inspected to confirm convergence. We use 100 Monte Carlo samples to produce gradient estimates. More details of the experiments are provided in Appendix D.

Diagnostics We measure the accuracy of our fitted variational density using two diagnostics based on importance sampling and described in Appendix E: ESS_e and \hat{k} .

Results Table 3 reports our results. All methods aside from gTAF achieve reasonable performance in terms of \hat{k} (below 0.7) in all settings. In terms of ESS_e , for $\nu = 30$ the best results are for mTAF, but all methods do well ($ESS_e > 0.7$). For heavier tails ($\nu \leq 2$), TTF fix has the best results in every case (with ESS_e at least 0.75). TTF produces slightly worse ESS_e values (with ESS_e at least 0.5). The values for mTAF and gTAF are worse than either TTF method, especially for the $\nu = 1, d = 50$ case ($ESS_e < 0.1$).

Overall the results show that, as before, it is advantageous to model tails in the final transformation (TTF, TTF fix). Fixing the tail parameters improves performance of TTF fix over TTF, but this is not consistently the case when comparing mTAF and gTAF.

5 Conclusion

Most current methods for modelling extremes with normalizing flows use heavy tailed base distributions. We demonstrate this can perform poorly, due to extreme inputs to neural networks causing slow convergence. We present an alternative: use a Gaussian base distribution and a final transformation which can induce heavy tails. We propose the TTF

d	Flow	$\nu = 1$		$\nu = 2$		$\nu = 30$	
		ESS_e	\hat{k}	ESS_e	\hat{k}	ESS_e	\hat{k}
5	gTAF	0.53	0.93	0.90	0.79	0.97	0.53
	TTF	0.83	0.40	0.89	0.43	0.98	0.18
	mTAF	0.10	0.18	0.52	-0.18	0.99	0.31
	TTF (fix)	0.97	0.37	0.98	0.35	0.98	0.19
10	gTAF	0.28	1.05	0.74	0.89	0.96	0.28
	TTF	0.90	0.36	0.92	0.36	0.96	0.20
	mTAF	0.09	0.31	0.52	-0.37	0.98	0.25
	TTF (fix)	0.93	0.33	0.95	0.32	0.97	0.07
50	gTAF	0.08	0.82	0.39	0.83	0.84	0.13
	TTF	0.57	0.25	0.61	0.24	0.79	0.14
	mTAF	0.02	0.57	0.41	0.03	0.90	0.17
	TTF (fix)	0.75	0.18	0.81	0.18	0.85	0.08

Table 3: Variational inference results for artificial target. Each entry is a mean value across 5 repeated experiments. For ESS_e columns, bold indicates the method with best value for each d . For \hat{k} columns, bold indicates any value below 0.7.

transformation, equation (3), and prove it can indeed produce heavy tails. In our examples, a version of our method, TTF fix, has the best performance overall. For examples with heavy tails it is usually the best performer, or if not it is within a standard error of it. It does not damage performance for examples without heavy tails. Here all types of NF we considered perform well.

More generally, the experimental results show that final transformation methods generally outperform heavy base methods. We also compare two stage and one stage methods. The former begin by estimating the tail parameters and then train the rest of the flow. TTF fix is an example of this. The latter train all flow parameters jointly. We find that two stage methods often outperform one stage methods, although in other examples there is no difference. Interestingly, another two stage final transformation method – COMET flows (McDonald et al., 2022)—often performs competitively, which we discuss further in Appendix F.

5.1 Limitations and Future Work

An arguable limitation of our transformation is that it **always** converts Gaussian tails to heavy tails. Hence it cannot produce exactly Gaussian tails. It is not clear whether this is detrimental in practice, and it does not prevent good performance in all our experiments.

Another potential limitation is that the TTF transformation affects both the body and tail of the output distribution. The preceding layers of the flow must learn to model the body of the distribution, and also adapt to the final layer. It would be appealing to decouple the transformations, so that they can concentrate separately on the body and tail, which

would hopefully make optimisation easier. This could be achieved by somehow ensuring the final transformation is approximately the identity in the body region.

Our final transformation converts each margin to a heavy tailed distribution. This is limiting, as the choice of directions to transform depends on an arbitrary choice of parameterisation. Future work could try to address this by using an autoregressive structure (Papamakarios et al., 2021) for the tail parameters for each marginal, or by adding a linear layer (e.g. that of Oliva et al., 2018) after our transformation.

Possible future work is to design methods which incorporate more extreme value theory properties. For instance, our method doesn't explicitly allow for tail dependence (Coles et al., 1999). This would be an interesting direction for future work, for instance by adapting the manifold copula method proposed by McDonald et al. (2022). Also, it would be interesting to design multivariate transformations with the max-stable property (Coles, 2001).

As mentioned above, our best experimental results are for a two stage method. A corresponding method for VI would be useful, such as using the static analysis method of Liang et al. (2024) to generate initial tail weight estimates. Also, it would be desirable to understand why a one stage method has worse performance, and try to improve this.

In this paper we've only included a proof-of-concept VI example on an artificial target. In exploratory work, we found it difficult to improve VI results on real examples using our method. One reason is that our experiments only show major improvements for sufficiently heavy tails (e.g. $\nu < 2$ in Tables 2, 3), which we found to be rare for real posteriors. The limitations of our transformation outlined above may also contribute.

Finally, a potential future application is to simulation based inference. Here neural likelihood estimation methods (Papamakarios et al., 2019) use density estimation with NFs to estimate a likelihood function from simulated data. Our approach could improve results when the simulated data is heavy tailed. More generally, our transformation may be useful to produce heavy tails with other generative models.

Acknowledgements Thanks to Miguel de Carvalho, Seth Flaxman, Iain Murray, Ioannis Papastathopoulos, Scott Sisson, Jenny Wadsworth and Peng Zhong for helpful discussions. Tennessee Hickling is supported by a PhD studentship from the EPSRC Centre for Doctoral Training in Computational Statistics and Data Science (COMPASS). A preliminary version of this work (Hickling and Prangle, 2023), using a similar transformation was presented to the MIDAS workshop at ECML-PKDD 2023.

Appendix A. TTF details

This appendix gives more details of our TTF transformation:

$$R(z; \lambda_+, \lambda_-) = \mu + \sigma \frac{s}{\lambda_s} [\operatorname{erfc}(|z|/\sqrt{2})^{-\lambda_s} - 1].$$

Recall that $s = \operatorname{sign}(z)$ and

$$\lambda_s = \begin{cases} \lambda_+ & \text{for } s = 1, \\ \lambda_- & \text{for } s = -1. \end{cases}$$

First, Section A.1 reviews some background on the complementary error function. Then Section A.2 presents a motivation for the transformation, and Section A.3 discusses some of its properties.

A.1 Complementary error function

For $z \in \mathbb{R}$, the error function and complementary error function are defined as

$$\begin{aligned} \operatorname{erf}(z) &= \frac{2}{\sqrt{\pi}} \int_0^z \exp(-t^2) dt, \\ \operatorname{erfc}(z) &= 1 - \operatorname{erf}(z). \end{aligned}$$

For large z , $\operatorname{erfc}(z) \approx 0$, so it can be represented accurately in floating point arithmetic.

Note that

$$F_N(z) = \frac{1}{2}(1 + \operatorname{erf}[z/\sqrt{2}]). \quad (5)$$

where $F_N(z)$ is the $\mathcal{N}(0, 1)$ cumulative distribution function. This implies

$$\operatorname{erfc}^{-1}(x) = -F_N^{-1}(x/2)/\sqrt{2}. \quad (6)$$

Efficient numerical evaluation of erfc and its gradient is possible, as it is a standard special function (Temme, 2010), implemented in many computer packages. For instance PyTorch provides the `torch.special.erfc` function. Later we also require erfc^{-1} , which is less commonly implemented directly. However using (6) we can compute erfc^{-1} using the more common standard normal quantile function F_N^{-1} . For instance PyTorch implements this as `torch.special.ndtri` (although this can have problems for small inputs—see Appendix D.3).

A.2 Motivation

This section motivates the TTF transformation by sketching how it can be derived from some simpler transformations. This gives an informal derivation that R transforms $\mathcal{N}(0, 1)$ tails to GPD tails. The formal version, Theorem 12, is presented later and also appropriately generalises the result to $\mathcal{N}(\mu, \sigma^2)$ inputs.

GPD transform Section 2.4 motivates the transformation $P : [0, 1] \rightarrow \mathbb{R}^+$ given by the GPD quantile function

$$P(u; \lambda) = \frac{1}{\lambda} [(1 - u)^{-\lambda} - 1], \quad (7)$$

where $\lambda > 0$ is the shape parameter. Using P transforms a distribution with support $[0, 1]$ to one on \mathbb{R}^+ with tunable tail weight.

We note that (7) is also valid for $\lambda < 0$ and maps $[0, 1]$ to $[0, \frac{1}{\lambda}]$. Here the image of the transformation depends on the parameter values, which is not a useful property for a normalizing flow. Hence we do not consider negative λ in our work.

Two tailed transform We can extend (7) to a transformation $Q : [-1, 1] \rightarrow \mathbb{R}$,

$$Q(u; \lambda_+, \lambda_-) = \frac{s}{\lambda_s} [(1 - |u|)^{-\lambda_s} - 1]. \quad (8)$$

Here $\lambda_+ > 0, \lambda_- > 0$ are shape parameters for the positive and negative tails. We use the notation $s = \text{sign}(u)$, with λ_s defined as earlier.

Using Q transforms a distribution with support $[-1, 1]$ to one on \mathbb{R} with tunable weights for both tails.

Real domain transform We would like a transformation $R : \mathbb{R} \rightarrow \mathbb{R}$ which can transform Gaussian tails to GPD tails. Consider $z \in \mathbb{R}$, and let $u = 2F_N(z) - 1$, where F_N is the $\mathcal{N}(0, 1)$ cumulative distribution function. Then $u \in [-1, 1]$ and we can output $Q(u)$. A drawback is that large $|z|$ can give u values which are rounded to ± 1 numerically.

Using (5) shows that

$$1 - |u| = \text{erfc}(|z|/\sqrt{2}), \quad (9)$$

so there is a standard special function to compute $1 - |u|$ directly. Large $|z|$ gives $1 - |u| \approx 0$, which can be represented to high accuracy in floating point arithmetic, avoiding the catastrophic rounding which could result from working directly with u .

Substituting (9) into (8) and adding location and scale parameters results in our TTF transformation R .

A.3 Properties

Here we derive several properties of the TTF transformation, R . These include expressions which are useful in an automatic differentiation implementation of R for normalizing flows: R^{-1} and derivatives of R and R^{-1} .

Forward transformation The derivative of R with respect to z is given by

$$\frac{\partial R}{\partial z}(z; \mu, \sigma, \lambda_+, \lambda_-) = \sigma \sqrt{\frac{2}{\pi}} \exp(-z^2/2) \text{erfc}(|z|/\sqrt{2})^{-\lambda_s - 1}. \quad (10)$$

All of these factors are positive, which implies that for all parameter settings $\frac{\partial R}{\partial z}(z) > 0$, so the transformation is monotonically increasing.

The transformation is continuously differentiable at $z = 0$ as

$$\frac{\partial R}{\partial z}(0; \mu, \sigma, \lambda_+, \lambda_-) = \sigma \sqrt{\frac{2}{\pi}}. \quad (11)$$

This has no dependence on the λ_+, λ_- and is the limit as $z \rightarrow 0$ from above or below.

Inverse transformation Define $y = \lambda_s |(x - \mu)/\sigma| + 1$. Then the inverse transformation is

$$R^{-1}(x; \mu, \sigma, \lambda_+, \lambda_-) = s\sqrt{2} \operatorname{erfc}^{-1}(y^{-1/\lambda_s}). \quad (12)$$

Note here we can take $s = \operatorname{sign}(x - \mu)$. The gradient is

$$\frac{\partial R^{-1}}{\partial x}(x; \mu, \sigma, \lambda_+, \lambda_-) = \frac{1}{\sigma} \sqrt{\frac{\pi}{2}} y^{-1/\lambda_s - 1} \exp\left(\operatorname{erfc}^{-1}(y^{-1/\lambda_s})^2\right). \quad (13)$$

Appendix B. Asymptotic results

This section proves asymptotic results on the tails produced by COMET flows and our TTF transformation. Our main aim is to prove whether or not the distributions are in the Fréchet domain of attraction Θ_λ (see Definition 3). We will also find the tail behaviour in detail for some special cases.

Throughout this section we use the following asymptotic notation. In particular, \sim is **not** used to describe probability distributions, as it is elsewhere in the paper.

Definition 4 For functions $f : \mathbb{R} \rightarrow \mathbb{R}^+$ and $g : \mathbb{R} \rightarrow \mathbb{R}^+$, we write

1. $f(x) = O(g(x))$ if $\limsup_{x \rightarrow \infty} f(x)/g(x) < \infty$,
2. $f(x) \sim g(x)$ if $\lim_{x \rightarrow \infty} f(x)/g(x) = 1$.

B.1 Background

The material in this section will be used in the proofs later in this appendix. The first results are on regularly varying functions, and based on the presentation in Nair et al. (2022).

Definition 5 A function $f : \mathbb{R}^+ \rightarrow \mathbb{R}^+$ is **regularly varying** of index $\rho \in \mathbb{R}$ if

$$\lim_{x \rightarrow \infty} f(kx)/f(x) = k^\rho$$

for all $k > 0$. When $\rho = 0$, $f(x)$ is **slowly varying**.

The following result is Lemma 2.7 of Nair et al.

Theorem 6 For slowly varying $f(x)$,

$$\lim_{x \rightarrow \infty} x^\rho f(x) = \begin{cases} 0 & \text{if } \rho < 0, \\ \infty & \text{if } \rho > 0. \end{cases}$$

The following result is Theorem 2.8 of Nair et al.

Theorem 7 A function $f : \mathbb{R}^+ \rightarrow \mathbb{R}^+$ is regularly varying of index ρ if and only if

$$f(x) = x^\rho \ell(x)$$

for some slowly varying ℓ .

The following result is an immediate corollary of Theorem 7.5(i) of Nair et al.

Theorem 8 *Consider a real-valued random variable X with density $q(x)$. Its distribution is in Θ_λ if and only if q is regularly varying of index $-1 - \lambda$.*

Finally, we present a result of Liang et al. (2022).

Definition 9 *Let $\overline{\mathcal{E}^2}$ be the set of random variables X such that for some $\alpha > 0$*

$$\Pr(|X| \geq x) = O(\exp[-\alpha x^2]).$$

Note that $\overline{\mathcal{E}^2}$ includes Gaussian distributions, and does not intersect with Θ_λ for any $\lambda > 0$.

The following result is a special case of Theorem 3.2 of Liang et al., and is a more precise extension of Theorem 2.

Theorem 10 *$\overline{\mathcal{E}^2}$ is closed under Lipschitz transformations.*

Of interest is a Gaussian base distribution transformed by a Lipschitz transformation, such as most standard normalizing flows. The result shows that the output is in $\overline{\mathcal{E}^2}$, and not the Fréchet domain of attraction.

B.2 COMET flow tails

Recall that COMET flows (McDonald et al., 2022), reviewed in Section 1.1, use a Gaussian base distribution followed by a generic normalizing flow. Then each component of the output is transformed by $h \circ g$, where g is the logistic transformation and h is a GPD quantile function. The following result describes the resulting tails.

Theorem 11 *Let Z be a real random variable with density $p(z)$. Define $X = h \circ g(Z)$ where*

$$g(z) = \frac{1}{1 + \exp(-z)}, \quad h(z) = \frac{1}{\lambda} \left[(1 - z)^{-\lambda} - 1 \right].$$

Let $p_N(z; \mu, \sigma^2)$ denote a $\mathcal{N}(\mu, \sigma^2)$ density. Then:

1. *$Z \in \overline{\mathcal{E}^2}$ (see Definition 9) implies $X \notin \Theta_\lambda$ (the Fréchet domain of attraction).*
2. *For $p(z) \sim p_N(z; 0, \sigma^2)$, X has density $q(x) \sim q_{LN}(x; 0, \lambda^2 \sigma^2)$, a log-normal density with location zero and scale $\lambda^2 \sigma^2$.*

Statement 1 implies that the tails produced by COMET flows are not suitably heavy tailed under most standard NFs. The argument is as follows. Recall that Jaini et al. (2020); Liang et al. (2022) give details showing that most standard NFs are Lipschitz. Theorem 10 shows that applying a Lipschitz transformation to a Gaussian base distribution produces a distribution in $\overline{\mathcal{E}^2}$. Then statement 1 shows that COMET flows do not map this to the Fréchet domain of attraction, which is the desired property by Definition 3.

Statement 2 shows that in one particular case, the resulting tails are log-normal. While the log-normal distribution is heavy tailed under Definition 1, it is not in the Fréchet domain of attraction (see e.g. Embrechts et al., 2013, Example 3.3.31). Hence it cannot capture the

full range of asymptotic tail behaviours. For instance, all moments exist for a log normal distribution but not for a GPD.

Proof Let $x = h(v), v = g(z)$. It's straightforward to derive that

$$z \sim \lambda^{-1} \log x, \tag{14}$$

$$x \sim \exp(\lambda z)/\lambda, \tag{15}$$

$$g'(z) \sim (\lambda x)^{-1/\lambda}, \tag{16}$$

$$h'(v) \sim (\lambda x)^{1+1/\lambda}. \tag{17}$$

The change of variables theorem gives

$$q(x) = \frac{p(z)}{|g'(z)||h'(v)|} = \frac{p(z)}{\lambda x}. \tag{18}$$

Statement 1 We'll prove the contrapositive: $X \in \Theta_\lambda$ implies $Z \notin \overline{\mathcal{E}^2}$.

By Theorems 7 and 8, $X \in \Theta_\lambda$ implies $q(x) = x^{-\lambda-1}\ell(x)$ with $\lambda > 0$ and slowly varying ℓ . Thus

$$\begin{aligned} p(z) &\sim q(x)\lambda x && \text{from (18)} \\ &= x^{-\lambda-1}\ell(x)\lambda x && \text{expression for } q(x) \\ &\sim \exp(-\lambda[\lambda+1]z)\lambda^{\lambda+2}x\ell(x). && \text{from (15)} \end{aligned}$$

Let $s(z) = \lambda(\lambda+1)\exp(-\lambda[\lambda+1]z)$. Then

$$\frac{p(z)}{s(z)} \sim Dx\ell(x),$$

with $D = \lambda^{\lambda+1}/(\lambda+1)$. By Theorem 6 this ratio converges to ∞ .

It follows that there exists z_0 such that $z > z_0$ implies $p(z) > s(z)$. Thus for $z > z_0$:

$$\Pr(Z > z) = \int_z^\infty p(t)dt > \int_z^\infty s(t)dt = \exp(-\lambda[\lambda+1]z).$$

This contradicts $\Pr(|Z| > z) = O(\exp[-\alpha z^2])$ for some $\alpha > 0$, so $Z \notin \overline{\mathcal{E}^2}$.

Statement 2 From (18), $q(x) \sim p_N(z; \mu, \sigma^2)/\lambda x$. Substituting in the Gaussian density and (14) gives

$$q(x) \sim r(x) = Ax^{-1+B} \exp[-C(\log x)^2],$$

where $A = \frac{1}{\lambda\sigma(2\pi)^{1/2}} \exp[-\frac{\mu^2}{2\sigma^2}]$, $B = \frac{\mu}{\lambda\sigma^2}$ and $C = \frac{1}{2\lambda^2\sigma^2} > 0$. For $\mu = 0$, $r(x)$ is a log-normal $LN(0, \lambda^2\sigma^2)$ density, as required. ■

Remark The proof of statement 1 suggests that Z with an exponential distribution would produce output in the Fréchet domain of attraction. This motivates using a Laplace distribution as a base distribution for a COMET flow. A drawback is the lack of smoothness of the Laplace density at the origin.

B.3 TTF tails

Our transformation R is defined in (3). Here we consider a simplified version $S : \mathbb{R}^+ \rightarrow \mathbb{R}^+$,

$$S(z; \lambda) = \frac{1}{\lambda} [\operatorname{erfc}(z/\sqrt{2})^{-\lambda} - 1]. \quad (19)$$

This modifies R by setting the location parameter to zero and scale parameter to one, and only considering the upper tail. To simplify notation it uses λ in place of λ_+ . We provide the following result on tails produced by this transformation.

Theorem 12 *Let Z be a random variable with density $p(z) \sim p_N(z; \mu, \sigma^2)$, a $\mathcal{N}(\mu, \sigma^2)$ density. Define $X = S(Z; \lambda)$. Then:*

1. *The distribution of X is in the Fréchet domain of attraction with shape parameter $\lambda\sigma^2$.*
2. *For $\mu = 0, \sigma = 1$, X has density $q(x) \sim q_{GPD}(x; \lambda, 2^{1/(2+1/\lambda)})$, a GPD density with shape parameter λ and scale $2^{1/(2+1/\lambda)}$ (see Definition 13 below.)*

The result for the lower tail is a simple corollary. Also, the result is unaffected by adding a final location and scale transformation—as in our full TTF transformation R —except that the latter will modify the scale parameter in statement 2.

As argued in Section 3.1, most NFs use a standard normal base distribution, and are capable of producing the identity transformation. So statement 2 of Theorem 12 shows that composing them with R can produce output which has heavy tails with parameterised weights. Statement 1 provides robustness: the result remains true when the input to R is a Gaussian with arbitrary location and scale parameters.

B.3.1 LEMMAS

Here we present two lemmas which are used in the proof of Theorem 12.

Definition 13 *A GPD with shape $\lambda > 0$, location 0, and scale $\sigma > 0$ has density*

$$q_{GPD}(x; \lambda, \sigma) = \frac{1}{\sigma} (1 + \lambda x/\sigma)^{-1-1/\lambda}.$$

Lemma 14 *For $k > 0$,*

$$kq_{GPD}(x; \lambda, 1) \sim q_{GPD}(x; \lambda, k^{-1/(2+1/\lambda)}).$$

The left hand side is a GPD density with scale 1, multiplied by a constant k . The lemma shows this is asymptotically equivalent to a GPD density with unchanged shape but modified scale.

Proof Observe that

$$\begin{aligned} q_{GPD}(x; \lambda, \sigma) &\sim \sigma^{-2-1/\lambda} (\lambda x)^{-1-1/\lambda} \\ \Rightarrow kq_{GPD}(x; \lambda, 1) &\sim k(\lambda x)^{-1-1/\lambda} \sim q_{GPD}(x; \lambda, k^{-1/(2+1/\lambda)}). \end{aligned}$$

■

Lemma 15 *Suppose $x = S(z; \lambda)$. Then for large x ,*

$$z = \left[\frac{2}{\lambda} \log(\lambda x + 1) \right]^{1/2} + o(1), \quad (20)$$

$$z^2 = \frac{2}{\lambda} \log(\lambda x + 1) - \log \log(\lambda x + 1) + \log \frac{\lambda}{\pi} + o(1). \quad (21)$$

Proof Let $F_N(\cdot)$ be the $\mathcal{N}(0, 1)$ cdf. The result is a corollary of the following asymptotic expansion from Fung and Seneta (2018) (for $p \rightarrow 0$)

$$F_N^{-1}(p) = -[-2 \log p - \log \log p^{-2} - \log 2\pi]^{1/2} \left(1 + O \left[\frac{\log |\log p|}{(\log p)^2} \right] \right).$$

By definition, $x = \frac{1}{\lambda} [\operatorname{erfc}(z/\sqrt{2})^{-\lambda} - 1]$. So $z = \sqrt{2} \operatorname{erfc}^{-1}(p)$ where $p = (1 + \lambda x)^{-1/\lambda}$. Using (6) gives $z = -F_N^{-1}(p/2)$. Hence we get

$$z = \left[\frac{2}{\lambda} \log(\lambda x + 1) \right]^{1/2} \left[1 + \frac{-\log \log(\lambda x + 1) + \log \frac{\lambda}{\pi} + o(1)}{\frac{2}{\lambda} \log(\lambda x + 1)} \right]^{1/2} \left(1 + O \left[\frac{\log \log(\lambda x + 1)}{[\log(\lambda x + 1)]^2} \right] \right).$$

Expanding the middle factor using a Taylor series and checking the order of the remaining terms gives (20). Squaring the asymptotic expansion for z and checking the order of terms gives (21). \blacksquare

Remark A consequence of (21) which we will use later is:

$$z^2 = \eta(x) - \log \eta(x) + o(1), \quad (22)$$

where $\eta(x) = \frac{2}{\lambda} \log(\lambda x + 1) + \log \frac{2}{\pi}$.

B.3.2 PROOF OF THEOREM 12

Let $x = S(z; \lambda)$. The change of variables theorem gives:

$$q(x) = p(z) / |S'(z; \lambda)|.$$

Recall that

$$p(z) \sim p_N(z; \mu, \sigma^2) = \frac{1}{(2\pi)^{1/2} \sigma} \exp \left[-\frac{1}{2\sigma^2} (z - \mu)^2 \right],$$

and from (10),

$$S'(z; \lambda) = \sqrt{\frac{2}{\pi}} \exp(-z^2/2) \operatorname{erfc}(z/\sqrt{2})^{-\lambda-1}.$$

Hence

$$q(x) \sim \frac{1}{2} r(z; \mu, \sigma) \operatorname{erfc}(z/\sqrt{2})^{\lambda+1},$$

where

$$r(z; \mu, \sigma) = \frac{1}{\sigma} \exp \left[-\frac{1}{2} \left\{ \frac{1}{\sigma^2} (z - \mu)^2 - z^2 \right\} \right].$$

Rearranging (19) gives $(1 + \lambda x)^{-1/\lambda} = \operatorname{erfc}(z/\sqrt{2})$. So

$$q(x) \sim \frac{1}{2} r(z; \mu, \sigma) (1 + \lambda x)^{-(1+1/\lambda)}. \quad (23)$$

Note that $r(z; 0, 1) = 1$. Then the proof of statement 2 concludes by applying Lemma 14 to (23).

The remainder of the proof is for statement 1, and uses capital letters to represent constants with respect to x . We have

$$\log r(z; \mu, \sigma) = \frac{1}{2}(1 - \sigma^{-2})z^2 + Az + B.$$

Using Lemma 15 gives

$$\log r(z; \mu, \sigma) = \frac{1}{\lambda}(1 - \sigma^{-2}) \log(\lambda x + 1) + C[\log(\lambda x + 1)]^{1/2} + D \log \log(\lambda x + 1) + E + o(1).$$

So

$$r(z; \mu, \sigma) = F(\lambda x + 1)^{(1 - \sigma^{-2})/\lambda} \exp \left\{ C[\log(\lambda x + 1)]^{1/2} \right\} [\log(\lambda x + 1)]^D (1 + o(1)).$$

Substituting into (23) gives

$$\begin{aligned} q(x) &\sim \frac{1}{2}(1 + \lambda x)^{-1 - \lambda^{-1} \sigma^{-2}} F \exp \left\{ C[\log(\lambda x + 1)]^{1/2} \right\} [\log(\lambda x + 1)]^D (1 + o(1)) \\ \Rightarrow q(x) &= x^{-1 - \lambda^{-1} \sigma^{-2}} \ell(x), \end{aligned}$$

where

$$\ell(x) = G \exp \left\{ C[\log(\lambda x + 1)]^{1/2} \right\} [\log(\lambda x + 1)]^D (1 + o(1))$$

can easily be checked to be a slowly varying function. Applying Theorems 7 and 8 shows that Y is in the Fréchet domain of attraction with shape $\lambda \sigma^2$ as required.

Appendix C. TTF Transform: Variations and Related Work

This appendix discusses variations on our TTF transform R , (3), and related work in the literature. For simplicity we compare to R with location zero and scale one.

An intuitively appealing alternative transformation which converts Gaussian tails to heavy tails is

$$R_{\text{cdf}} = F_T^{-1} \circ F_N$$

where F_T and F_N are cdfs of Student's T and Gaussian distributions (both with location zero and scale one). Rather than use the Student's T distribution for the base distribution, as in the prior work reviewed in Section 1.1.2, this moves the use of the T distribution to the final transformation. Unfortunately, R_{cdf} is not practical as F_T^{-1} does not have a closed form allowing automatic differentiation.

Another alternative transformation is

$$R_{\text{alt}}(z; \lambda_+, \lambda_-) = \frac{s}{\lambda_s} \left[\left\{ \frac{1}{2} \operatorname{erfc}(|z|/\sqrt{2}) \right\}^{-\lambda_s} - 1 \right].$$

This only differs from our TTF transform in that a factor of $1/2$ has been included. Equation 3.15 of Shaw et al. (2014) shows that for $z \rightarrow \infty$, R_{alt} is asymptotically equivalent to R_{cdf} . Hence R_{alt} converts $\mathcal{N}(0, 1)$ tails to GPD tails. In this case it has the advantage of

producing output with scale one, which the TTF transformation does not do (see Theorem 12, statement 2). However, the reason we don't use R_{alt} is due to a disadvantage—there can be a discontinuity at $z = 0$, since

$$\begin{aligned}\lim_{z \rightarrow 0_+} R_{\text{alt}}(z; \lambda_+, \lambda_-) &= (2^{\lambda_+} - 1)/\lambda_+, \\ \lim_{z \rightarrow 0_-} R_{\text{alt}}(z; \lambda_+, \lambda_-) &= (2^{\lambda_-} - 1)/\lambda_-.\end{aligned}$$

Another related result is from Troshin (2022). This paper investigates necessary and sufficient conditions for transformations to map $\mathcal{N}(0, 1)$ inputs to the Fréchet domain of attraction. This produces a family of functions which includes R and R_{alt} —see Troshin's Remark 2. However, unlike our Appendix B, this work does not provide results for $\mathcal{N}(\mu, \sigma^2)$ inputs.

Appendix D. Implementation Details

This appendix contains more details of how we implement our experiments in Section 4 of the main paper.

D.1 Normalizing Flows

We use the `nflows` package (Durkan et al., 2020) to implement the NF models. This depends on PyTorch (Paszke et al., 2019) for automatic differentiation.

Our NF layers (autoregressive rational quadratic spline layer, and autoregressive affine layers) output the required transformation parameters from masked neural networks. These use 2 hidden layers, each with a width equal to the input dimension plus 10.

D.2 Sampling Student's T

Let t_ν represent a Student's T distribution with ν degrees of freedom. Algorithm 1 draws samples, while allowing the reparameterization trick i.e. differentiation with respect to ν .

Algorithm 1 Sampling Student's T

- Input: degrees of freedom ν , threshold $\epsilon \geq 0$.
- 1: Sample $g \sim \text{Gamma}(\nu/2, 1)$.
 - 2: Let $g' = \max(g, \epsilon)$.
 - 3: Sample $z \sim \mathcal{N}(0, 1)$.
 - 4: Return $z \sqrt{\frac{\nu}{2g'}}$.
-

Abiri and Ohlsson (2019) suggest this algorithm with $\epsilon = 0$, and comment on how to differentiate through a Gamma distribution. This method is implemented in PyTorch. However we found that taking the reciprocal of $g \approx 0$ can result in an overflow error. Hence we make a slight adjustment for numerical stability: we clamp g to $\epsilon = 1\text{e-}24$.

D.3 Inverse Transformation for Small Inputs

Equation (12) gives an expression for $R^{-1}(x)$, the inverse of our TTF transformation R , in terms of $\operatorname{erfc}^{-1}(y^{-1/\lambda_s})$ where $y(x) = \lambda_s|(x - \mu)/\sigma| + 1$. However we experience numerical issues when implementing (12) for small x . Therefore for $y^{-1/\lambda_s} < 10^{-6}$ our code uses the approximation

$$\widehat{R}^{-1}(x) = s [\eta(x) - \log \eta(x)]^{\frac{1}{2}},$$

where $\eta(x) = \frac{2}{\lambda_s} \log y(x) + \log \frac{2}{\pi},$

and $s = \operatorname{sign}(x - \mu)$. We have $\widehat{R}^{-1}(x) \approx R^{-1}(x)$ using (22).

Appendix E. Variational Inference Diagnostics

We measure the quality of a density $q_x(x)$ produced by VI using diagnostics based on importance sampling. This involves calculating $w_i = p(x_i)/q_x(x_i)$ where $p(x)$ is the target density and $x_i \sim q_x(x)$ (independently) for $i = 1, 2, \dots, n$. In our examples we use $n = 10,000$.

Our first diagnostic is based on effective sample size (Robert and Casella, 2004)

$$ESS(n) = \left(\sum_{i=1}^n w_i \right)^2 / \sum_{i=1}^n w_i^2.$$

We report ESS efficiency, $ESS_e(n) = ESS(n)/n$. A value of $ESS_e(n) \approx 1$ indicates $q_x(x) \approx p(x)$.

Our second diagnostic is from Yao et al. (2018), who fit a GPD to the w_i s and return the estimated shape parameter \hat{k} . Lower \hat{k} values indicate a better approximation of $p(x)$ by $q_x(x)$. Yao et al. (2018) argue that $\hat{k} > 0.7$ corresponds to a very poor approximation, and $\hat{k} < 0.5$ indicates a good fit.

Appendix F. Further Discussion of COMET Flows

Performance Where we can implement COMET flows in our empirical comparisons, they are competitive with the best performing methods—see Table 2. However our theory in Appendix B.2 shows they can’t capture all heavy tails, in one case producing log-normal tails rather than GPD tails. One possible reason for good empirical behaviour is that log-normal and GPD distributions have similar sub-asymptotic properties (Nair et al., 2022).

Limitations In our density estimation example on synthetic data (Section 4.2), we found that COMET flows were too slow to implement for $d = 50$. It’s unclear if the issue is fundamental to the method or due to its implementation. For instance, the existing implementation requires repeatedly moving data between the CPU and GPU, so a more efficient implementation might be more competitive.

We also found some bugs in the existing implementation of COMET flows, which are fixed in the code for our paper.

COMET flows involve an initial stage of KDE estimation of marginal distributions. This is not usually possible for VI, so the method is not generally applicable there.

References

- Najmeh Abiri and Mattias Ohlsson. Variational auto-encoders with Student’s t-prior. In *ESANN 2019 - Proceedings*, pages 837–848. ESANN, 2019.
- Saba Amiri, Eric T. Nalisnick, Adam Belloum, Sander Klous, and Leon Gommans. Generating heavy-tailed synthetic data with normalizing flows. In *The 5th Workshop on Tractable Probabilistic Modeling*, 2022.
- David M. Blei, Alp Kucukelbir, and Jon D. McAuliffe. Variational inference: A review for statisticians. *Journal of the American Statistical Association*, 112(518):859–877, 2017.
- Pasquale Cirillo and Nassim Nicholas Taleb. Tail risk of contagious diseases. *Nature Physics*, 16:606–613, 2020.
- Stuart Coles. *An Introduction to Statistical Modeling of Extreme Values*. Springer London, London, 2001. ISBN 978-1-84996-874-4.
- Stuart Coles, Janet Heffernan, and Jonathan Tawn. Dependence measures for extreme value analyses. *Extremes*, 2:339–365, 1999.
- Jon Danielsson, Laurens de Haan, Liang Peng, and Casper G. de Vries. Using a bootstrap method to choose the sample fraction in tail index estimation. *Journal of Multivariate analysis*, 76(2):226–248, 2001.
- Miguel de Carvalho, Soraia Pereira, Paula Pereira, and Patrícia de Zea Bermudez. An extreme value Bayesian lasso for the conditional left and right tails. *Journal of Agricultural, Biological and Environmental Statistics*, pages 1–18, 2022.
- Conor Durkan, Artur Bekasov, Iain Murray, and George Papamakarios. Neural spline flows. In *Advances in Neural Information Processing Systems*, volume 32, 2019.
- Conor Durkan, Artur Bekasov, Iain Murray, and George Papamakarios. nflows: normalizing flows in PyTorch, November 2020. URL <https://github.com/bayesiains/nflows>.
- Paul Embrechts, Claudia Klüppelberg, and Thomas Mikosch. *Modelling extremal events: for insurance and finance*. Springer Science & Business Media, 2013.
- Sergey Foss, Dmitry Korshunov, and Stan Zachary. *An introduction to heavy-tailed and subexponential distributions*. Springer, 2011.
- Thomas Fung and Eugene Seneta. Quantile function expansion using regularly varying functions. *Methodology and Computing in Applied Probability*, 20:1091–1103, 2018.
- Manfred Gilli and Evis Këllezi. An application of extreme value theory for measuring financial risk. *Computational Economics*, 27:207–228, 2006.
- Tennessee Hickling and Dennis Prangle. Flexible tails for normalising flows, with application to the modelling of financial return data. *arXiv preprint arXiv:2311.00580*, 2023.

- Bruce M. Hill. A simple general approach to inference about the tail of a distribution. *The Annals of Statistics*, 3(5), September 1975.
- Raphaël Huser, Thomas Opitz, and Jennifer Wadsworth. Modeling of spatial extremes in environmental data science: Time to move away from max-stable processes. *arXiv preprint arXiv:2401.17430*, 2024.
- Priyank Jaini, Ivan Kobyzev, Yaoliang Yu, and Marcus Brubaker. Tails of Lipschitz triangular flows. In *Proceedings of the 37th International Conference on Machine Learning*, volume 119, pages 4673–4681. PMLR, 2020.
- Ivan Kobyzev, Simon J. D. Prince, and Marcus A. Brubaker. Normalizing flows: An introduction and review of current methods. *IEEE transactions on pattern analysis and machine intelligence*, 43(11):3964–3979, 2020.
- Mike Laszkiewicz, Johannes Lederer, and Asja Fischer. Marginal tail-adaptive normalizing flows. In *International Conference on Machine Learning*, volume 162, pages 12020–12048. PMLR, 2022.
- Feynman T. Liang, Liam Hodgkinson, and Michael W. Mahoney. Fat-tailed variational inference with anisotropic tail adaptive flows. In *International Conference on Machine Learning*, volume 162, pages 13257–13270. PMLR, 2022.
- Feynman T. Liang, Liam Hodgkinson, and Michael W. Mahoney. A heavy-tailed algebra for probabilistic programming. *Advances in Neural Information Processing Systems*, 36, 2024.
- Andrew McDonald, Pang-Ning Tan, and Lifeng Luo. COMET flows: Towards generative modeling of multivariate extremes and tail dependence. In *International Joint Conference on Artificial Intelligence*, 2022.
- Kevin P. Murphy. *Probabilistic Machine Learning: Advanced Topics*. MIT Press, 2023.
- Jayakrishnan Nair, Adam Wierman, and Bert Zwart. *The fundamentals of heavy tails: Properties, emergence, and estimation*. Cambridge University Press, 2022.
- Philippe Naveau, Raphael Huser, Pierre Ribereau, and Alexis Hannart. Modeling jointly low, moderate, and heavy rainfall intensities without a threshold selection. *Water Resources Research*, 52(4):2753–2769, apr 2016.
- Junier Oliva, Avinava Dubey, Manzil Zaheer, Barnabas Poczos, Ruslan Salakhutdinov, Eric Xing, and Jeff Schneider. Transformation autoregressive networks. In *International Conference on Machine Learning*, volume 80, pages 3898–3907. PMLR, 2018.
- George Papamakarios, Theo Pavlakou, and Iain Murray. Masked autoregressive flow for density estimation. In *Advances in Neural Information Processing Systems*, volume 30, 2017.
- George Papamakarios, David Sterratt, and Iain Murray. Sequential neural likelihood: Fast likelihood-free inference with autoregressive flows. In *The 22nd International Conference on Artificial Intelligence and Statistics*, pages 837–848. PMLR, 2019.

- George Papamakarios, Eric Nalisnick, Danilo Jimenez Rezende, Shakir Mohamed, and Balaji Lakshminarayanan. Normalizing flows for probabilistic modeling and inference. *Journal of Machine Learning Research*, 22(57):1–64, 2021.
- Ioannis Papastathopoulos and Jonathan A. Tawn. Extended generalised Pareto models for tail estimation. *Journal of Statistical Planning and Inference*, 143(1):131–143, 2013.
- Adam Paszke, Sam Gross, Francisco Massa, Adam Lerer, James Bradbury, Gregory Chanan, Trevor Killeen, Zeming Lin, Natalia Gimelshein, Luca Antiga, Alban Desmaison, Andreas Kopf, Edward Yang, Zachary DeVito, Martin Raison, Alykhan Tejani, Sasank Chilamkurthy, Benoit Steiner, Lu Fang, Junjie Bai, and Soumith Chintala. Pytorch: An imperative style, high-performance deep learning library. In *Advances in Neural Information Processing Systems 32*, pages 8024–8035. Curran Associates, Inc., 2019.
- James Pickands III. Statistical inference using extreme order statistics. *The Annals of Statistics*, pages 119–131, 1975.
- Yongcheng Qi. Bootstrap and empirical likelihood methods in extremes. *Extremes*, 11: 81–97, 2008.
- Danilo Rezende and Shakir Mohamed. Variational inference with normalizing flows. In *International conference on machine learning*, volume 37, pages 1530–1538. PMLR, 2015.
- C.P. Robert and G. Casella. *Monte Carlo statistical methods*. Springer Verlag, 2004.
- William T. Shaw, Thomas Luu, and Nick Brickman. Quantile mechanics ii: changes of variables in Monte Carlo methods and GPU-optimised normal quantiles. *European Journal of Applied Mathematics*, 25(2):177–212, January 2014. ISSN 1469–4425. doi: 10.1017/s0956792513000417. URL <http://dx.doi.org/10.1017/s0956792513000417>.
- Michael L. Stein. Parametric models for distributions when interest is in extremes with an application to daily temperature. *Extremes*, 24(2):293–323, 2021.
- Nico M. Temme. Error functions, Dawson’s and Fresnel integrals. In *NIST handbook of mathematical functions*. Cambridge university press, 2010.
- V. V. Troshin. On the maximum domain of attraction for transformations of a normal random variable. *Journal of Mathematical Sciences*, 262(4):537–543, 2022.
- Jun Yang, Krzysztof Łatuszyński, and Gareth O. Roberts. Stereographic Markov chain Monte Carlo. *arXiv preprint arXiv:2205.12112*, 2022.
- Yuling Yao, Aki Vehtari, Daniel Simpson, and Andrew Gelman. Yes, but did it work?: Evaluating variational inference. In *Proceedings of the 35th International Conference on Machine Learning*, volume 80, pages 5581–5590. PMLR, 2018.
- Jingzhao Zhang, Sai Praneeth Karimireddy, Andreas Veit, Seungyeon Kim, Sashank Reddi, Sanjiv Kumar, and Suvrit Sra. Why are adaptive methods good for attention models? In H. Larochelle, M. Ranzato, R. Hadsell, M.F. Balcan, and H. Lin, editors, *Advances in Neural Information Processing Systems*, volume 33, pages 15383–15393. Curran Associates, Inc., 2020.

Jakob Zscheischler, Seth Westra, Bart van den Hurk, Sonia Isabelle Seneviratne, Philip J. Ward, Andrew J. Pitman, Amir Aghakouchak, David N. Bresch, Michael Leonard, Thomas Wahl, and Xuebin Zhang. Future climate risk from compound events. *Nature Climate Change*, 8:469–477, 2018.